2021

Effect of head size and rotation on taper corrosion in a hip simulator

C. M. Wight

C. M. Whyne

E. R. Bogoch

R. Zdero

Ryan M. Chapman

See next page for additional authors

Effect of head size and rotation on taper corrosion in a hip simulator

Authors

C. M. Wight, C. M. Whyne, E. R. Bogoch, R. Zdero, Ryan M. Chapman, D. W. van Citters, W. R. Walsh, and E. Schemitsch

Creative Commons License

This work is licensed under a Creative Commons Attribution-Noncommercial-No Derivative Works 4.0 License.

Follow us @BoneJointOpen

Freely available online OPEN ACCESS

HIP

Effect of head size and rotation on taper corrosion in a hip simulator

C. M. Wight,
C. M. Whyne,
E. R. Bogoch,
R. Zdero,
R. M. Chapman,
D. W. van Citters,
W. R. Walsh,
E. Schemitsch

From University of Toronto, Toronto, Ontario, Canada

Aims

This study investigates head-neck taper corrosion with varying head size in a novel hip simulator instrumented to measure corrosion related electrical activity under torsional loads.

Methods

In all, six 28 mm and six 36 mm titanium stem-cobalt chrome head pairs with polyethylene sockets were tested in a novel instrumented hip simulator. Samples were tested using simulated gait data with incremental increasing loads to determine corrosion onset load and electrochemical activity. Half of each head size group were then cycled with simulated gait and the other half with gait compression only. Damage was measured by area and maximum linear wear depth.

Results

Overall, 36 mm heads had lower corrosion onset load (p = 0.009) and change in open circuit potential (OCP) during simulated gait with (p = 0.006) and without joint movement (p = 0.004). Discontinuing gait's joint movement decreased corrosion currents (p = 0.042); however, wear testing showed no significant effect of joint movement on taper damage. In addition, 36 mm heads had greater corrosion area (p = 0.050), but no significant difference was found for maximum linear wear depth (p = 0.155).

Conclusion

Larger heads are more susceptible to taper corrosion; however, not due to frictional torque as hypothesized. An alternative hypothesis of taper flexural rigidity differential is proposed. Further studies are necessary to investigate the clinical significance and underlying mechanism of this finding.

Cite this article: *Bone Jt Open* 2021;2-11:1004–1016.

Keywords: Fretting, Corrosion, Hip simulator, Metal-on-polyethylene, Total hip arthroplasty, Frictional torque

Introduction

Larger femoral heads (≥ 36 mm) may be preferred in metal-on-polyethylene total hip arthroplasty (THA) to reduce the risk of dislocation by increasing the impingement free range of motion (ROM) and jump distance of the head from the cup.[1] However, large head size has been implicated in contributing to head-neck taper corrosion.[2] Severe taper corrosion led to the market withdrawal of many large diameter metal-on-metal THA constructs.[3] However, retrieval analyses have reported mixed results regarding the contribution of head diameter to taper corrosion in metal-on-polyethylene prostheses.[4-6] Some surgeons have cautioned against femoral heads ≥ 36 mm, even in polyethylene acetabular liners, until the issue is better understood.[7]

The mechanism underlying the impact large heads have on head-neck taper corrosion is not well understood. One hypothesis is that larger heads provide a greater moment arm for forces generated by articular friction causing greater torque at the taper connection (Figure 1). Jauch et al[8] showed torsion less than that found from friction in metal-on-crosslinked polyethylene bearings (3.92 Nm vs 9 Nm)[9] can initiate taper fretting corrosion.

The use of retrieval analyses is challenged by a diverse patient population, in terms of both physiological and device design parameters, towards understanding the impact of head size on taper corrosion. A highly

Correspondence should be sent to Christian M Wight; email: christian.wight@mail.utoronto.ca

doi: 10.1302/2633-1462.211.BJO-2021-0147.R1

Bone Jt Open 2021;2-11:1004–1016.

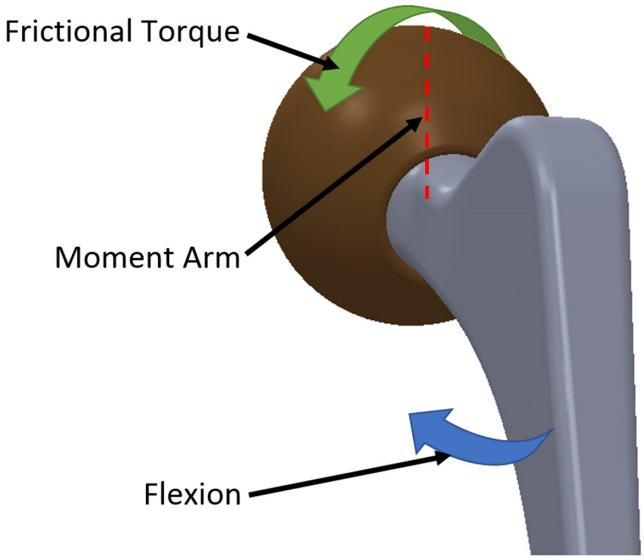

Fig. 1

Frictional torque induced by femoral head rotation within an acetabular cup (green) during flexion (blue) is proportionate to the moment arm (red) from the head's outer spherical surface to the trunnion's central axis. The moment arm increases with femoral head size as the head's outer surface moves further from the trunnion's central axis.

controlled in vitro bench-top study could strengthen the body of evidence by investigating head size as the single independent variable in a test apparatus approximating in-vivo conditions. Yet despite potential contribution from torque, the standard taper corrosion test method (ASTM F1875[1])[10] requires only uni-axial cyclic compressive loading, without joint movement that would generate frictional torque. Therefore, a novel hip simulator instrumented to measure corrosion related electrical activity is needed to quantify the effect of clinically relevant frictional torque on taper corrosion.

The aims of this study were to develop a novel instrumented hip simulator test apparatus to determine the role of rotational joint movements in head-neck taper corrosion, and investigate the susceptibility to and severity of taper corrosion with increasing head diameter in a metal-on-polyethylene articulation. It is hypothesized that the samples subject to joint movement will exhibit greater taper damage and that this effect will be greater with larger femoral head samples.

Methods

Materials. Femoral test samples were implant grade final products (Synergy Stem; Smith & Nephew, UK; Figure 2). Femoral heads were Co-Cr-Mo alloy (CoCr), with either 28 mm or 36 mm diameter, and all neutral offset (0 mm) to ensure no taper coverage or offset differences. Femoral neck samples were prepared from Ti-6Al-4V alloy femoral stems. Stems were cut 15 mm below the resection level, and two tapped holes were added to the sectioned surface to allow test apparatus connection. Femoral neck

Fig. 2

Synergy Stem and CoCr femoral head test samples (Smith & Nephew, UK).

samples were embedded to the resection level in Ortho-Jet BCA acrylic resin (Lang Dental, USA). Modifying the stem this way is considered acceptable because in-vivo stems are also often biologically fixed by bony ingrowth to the resection level, such that the stem's flexural rigidity in the region around the taper connection is equivalent to the test samples. Acetabular samples were manufactured

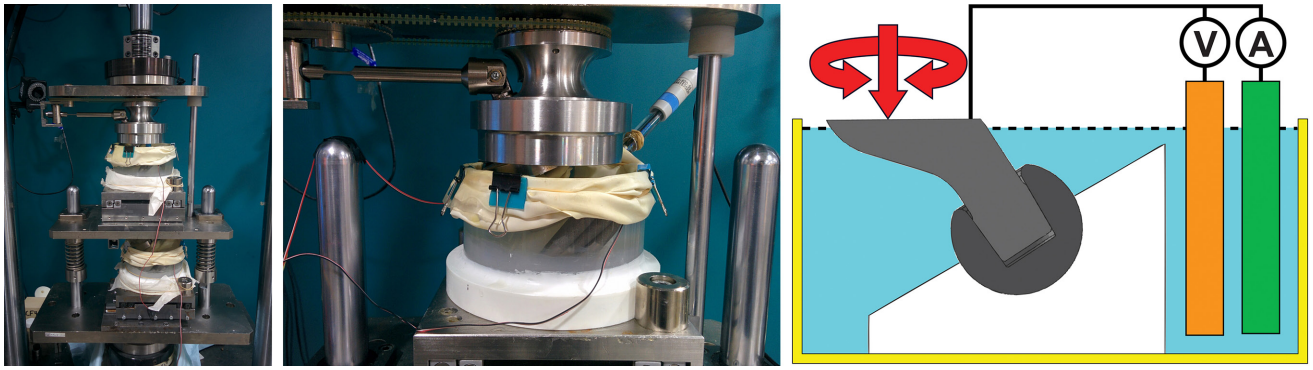

Fig. 3

Modified dual station hip simulator (left), instrumented upper module (centre) and schematic (right) illustrating the test sample (grey) and polyethylene socket (white) in a saline (blue) filled test chamber (yellow) with flexible cap (dotted line) containing reference electrode (orange) and counter electrode (green) connected to the test sample and subject to applied load (red).

from non-crosslinked UHMWPE rod (ASTM F648) with a 30° angled top surface to simulate anatomical head coverage and a central spherical cavity to mate with the 28 mm or 36 mm head. Angulation of the acetabular sample mimics the orientation and head coverage in-vivo. Six samples of each head size were tested to allow practical test duration and a minimum of three samples per head size and wear test loading regime.

Apparatus. The test apparatus is a modified BioPuls Dual Station ASTM Hip Simulator (Instron, USA), as depicted in Figure 3. The hip simulator is connected to a calibrated bi-axial servohydraulic test frame (MTS, USA) including upper and lower modules. The test frame applies identical compression to the upper and lower modules. The upper module includes a mechanism that translates the test frame's single rotation axis into coordinated 3° of freedom flexion-extension, internal-external rotation, and abduction-adduction of simulated gait via a series of interconnected and offset gears. As a result, under the hip simulator's intended use, the upper module wear tests samples under compression and joint movement, whereas the lower module is for load-soaked control samples subject only to compression.

The simulator was modified to allow connection of test samples, electronically isolating the samples and connecting them to electrical measuring equipment. Test samples were connected to the hip simulator via custom manufactured sample holders. Samples were isolated by excluding all extraneous metal components from the test solution. Test samples were contained in a custom manufactured test chamber made of high-density polyethylene, polycarbonate and silicone sealant topped with a latex membrane. The polyethylene acetabular liners were connected to the test chamber's base by screws isolated by an O-ring and silicone sealant. The femoral sample holder was isolated from the rest of the hip simulator via a sleeve made of polymer, and only the femoral neck and head entered the test chamber. In between tests, the test chamber was thoroughly cleaned to prevent third body wear.

Test samples were connected to an Ag/AgCl reference electrode (Accumet; Fisher Scientific, USA) through a Keithley 6514 electrometer (Keithley Instruments, USA) to measure the sample's open circuit potential (OCP). Test samples were also connected to a Ti-6Al-4V counter electrode through a Keithley 6485 picoammeter (Keithley Instruments) to measure the corrosion current. The counter electrode was manufactured from remnant distal tips after sectioning the stem samples.

The apparatus for the lower module mirrors the upper module, excluding sample holder modification since joint movement was not necessary.

Methods

Prior to testing, samples were ultrasonically cleaned using Alconox detergent (Alconox, USA) in accordance with the detergent manufacturer's instructions and visually inspected for baseline characterization. Samples were assembled under wet conditions to generate a challenge condition compared to dry assembly.[9] The femoral head's bore was filled with phosphate buffered saline (PBS) and the femoral neck's trunnion was pressed into the head with a servohydraulic test frame (MTS, USA) applying 2 kN axial load at a rate of 0.5 kN/s in accordance with ISO 7206-10.[10] Assembled components were then placed in individual PBS filled sample containers for 72 hours to electrochemically stabilize the system before testing. During this period the samples' passive oxide layers reach equilibrium within the test environment such that minimal electrochemical activity takes place.

All samples were subjected to simulated gait with a periodically increasing incremental peak load. Simulated gait follows a double peak compressive load pattern per ISO 14242-1[11] and sinusoidal 19° rotation applied by the test frame, which translates to standard deviation (SD) 10° flexion/extension, SD 2.5° abduction/adduction,

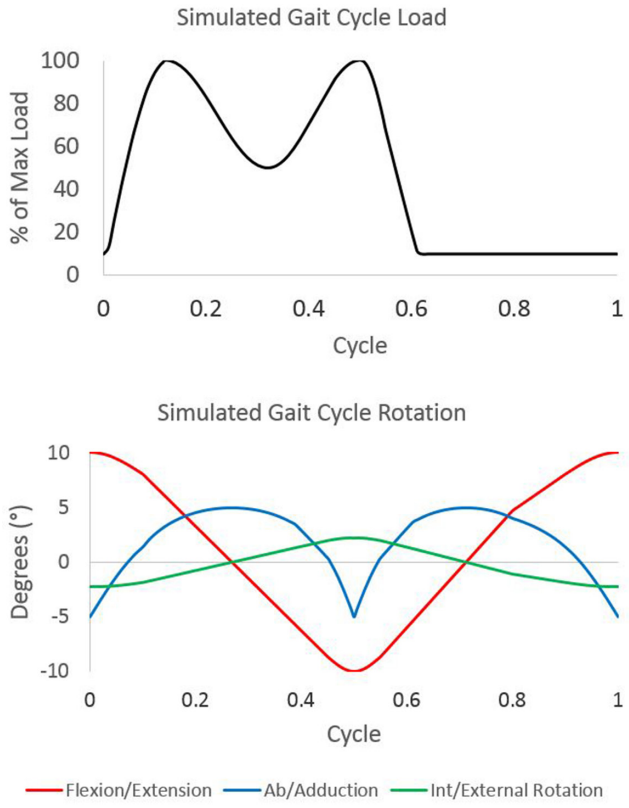

Fig. 4
Simulated gait cycle load and rotation.

and SD 2° internal/external rotation (Figure 4). The peak load increments rose from 100 N steps from 100N to 1,100N, to 200 N steps from 1,100 N to 3,300 N, while maintaining a 0.1 minimum to maximum load ratio. Cyclic loading was continued at each increment for three minutes, then OCP and corrosion current were measured before proceeding to the next load. After measurements were taken at 3,300 N compression with joint movement, joint movement was discontinued and OCP and corrosion current were measured after three minutes of cyclic compression only.

Corrosion onset load was determined by identifying the load where both OCP and corrosion current first increased from baseline as determined visually from a plot and confirmed via fast fourier transformation of current data to identify the load corresponding to a 3 Hz cyclic behaviour. This early electrical activity is considered the corrosion process's initiation that may lead to observable taper damage over time. Corrosion current and change in OCP from baseline measured at 3,300 N cycling with and without joint movement are also considered as surrogates for corrosion, with higher values indicating greater corrosion on the basis that each corrosion reaction releases a certain number of ions and with more corrosion reactions more ions would be measured as electrical activity.

After incremental gait loading, half of each group (28 mm and 36 mm) was long-term wear cycled in either the hip simulator's upper or lower module. Samples cycled in the upper module were subject to full simulated gait, with double peak compression to maximum 3,300 N and joint movement as described above, at a rate of 3 Hz. The cycling frequency is greater than 1 Hz typical of simulated gait[11] and as recommended by ASTM F1875 for taper connection electrochemical characterization.[12] However, the cycling frequency is aligned with ASTM F1875[10] recommendations for long term taper connection fretting corrosion testing at frequencies below 5 Hz, and an in vitro study by Brown et al[13] who observed corrosion currents at loading frequencies up to 10 Hz. The lower module was subject only to identical compression loading, without joint movement. Samples tested in the lower module were held in the neutral orientation per ISO 14242-1.[11] All samples were cycled for one million cycles.

At the completion of wear cycling, femoral heads were disassembled via tensile axial distractive load. Taper surfaces were rinsed and gently wiped with non-abrasive cloth to remove adherent debris. Material loss from the head tapers was measured via ccoordinate measuring machine (CMM) by an experienced laboratory following a previously validated technique.[14] Material loss from the stem tapers was not measured because the entirety of the trunnion was assembled within the head so no pristine surface after testing could be identified. Measurements were taken using a Zeiss Contura G2 CMM running Calypso software (Oberkochen, Germany). Heads were mounted at four points around the equator using a non-marring fixture. A custom measurement script was used to take at least 72 axial scans along the length of the head taper capturing 3D position every 0.1 mm with a 3 mm ruby stylus.

The measured point clouds were analyzed using Matlab (USA). Data was presented in graphical form and the evaluator selected a reference unworn region from which the original as-machined surface was extrapolated and material loss calculated. Material loss was presented as the maximum linear deviation from the as-machined surface. All devices were independently measured and analyzed three times by a single operator. The technique is accurate and repeatable to better than 7 µm for any retrieved bore.[14] For this study, the measure's 95% confidence interval was calculated to be 2 µm. The accuracy and repeatability reported considers all sources of error, including CMM measurement error, 3D reconstruction error, and variability between operators.

Femoral head tapers were then visually inspected to identify wear mechanisms and measure the fretting and/or corrosion damage surface areas. Damaged surface areas were measured by image analysis using Illustrator software (Adobe, USA). Images of the stem and head

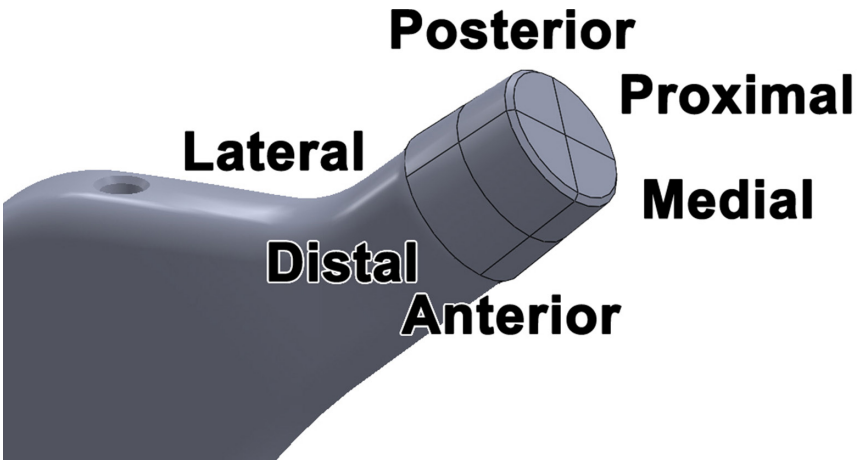

Fig. 5

Definition of taper regions by dividing into quarters corresponding to medial, lateral, anterior, and posterior aspects, and dividing into proximal and distal halves. Head taper regions match stem taper regions.

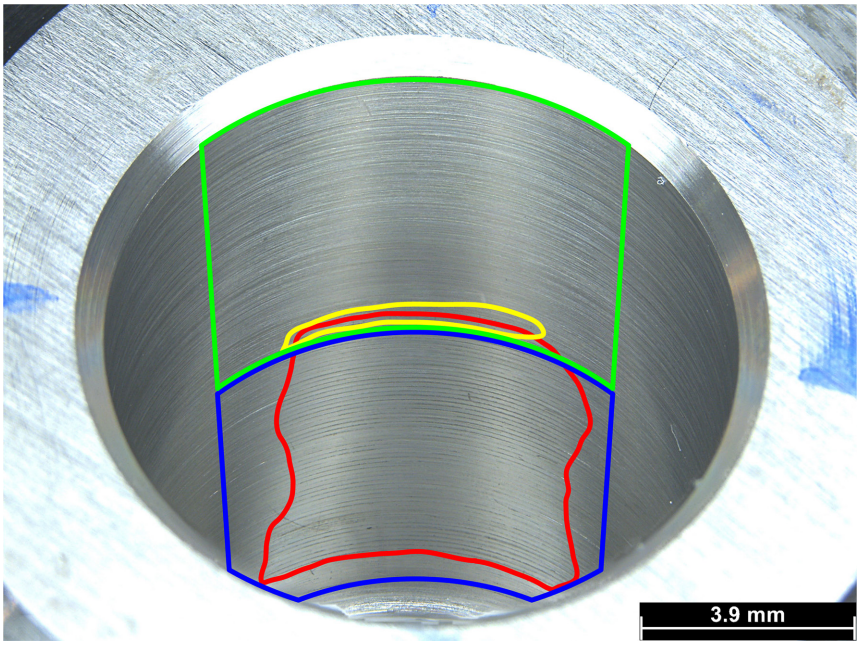

Fig. 6

Example fretting and corrosion damage area identification. A stereomicroscopic image is taken of the head taper's medial aspect and proximal (blue) and distal (red) regions of interest are identified. Within the regions of interest, fretting (yellow) and corrosion (red) damaged regions are manually traced. Area of the traced regions are calculated using a standard software function (Adobe Illustrator, USA).

taper's medial, lateral, anterior and posterior aspects were taken using a Leica M123C stereomicroscope (Leica Microsystems, Germany) with the Leica LAS X software's Z-stack feature to ensure a focused image down the head's bore. Images were loaded into Illustrator software and the region of interest was identified geometrically corresponding to a 90° arc centred on the image. Each region was further divided into proximal and distal halves (Figure 5). Regions of fretting or corrosion were outlined using Adobe Illustrator's pen tool and the area was calculated using the path area command (Figure 6). The areas on each aspect were summed to calculate the total corrosion or fretting damaged areas.

Statistical analysis. Statistical analysis was performed using SPSS 26 (IBM, USA). Data collected during the incremental load test was analyzed by analysis of variance (ANOVA) with Tukey post-hoc analysis to determine the effect of head size. Corrosion current, change in OCP at cycling initiation (0 N to 100 N), and change in OCP at 3,300 N peak loading with and without joint movement were each compared via paired *t*-test. Fretting and corrosion area comparisons were completed via paired

Table I. Incremental load test electrochemical measurements.

Parameter	28 mm head, mean (SD)	36 mm head, mean (SD)
Corrosion onset load, N*	1,800 (330)	1,250 (250)
Change in OCP† at 100 N with joint movement, mV	21.88 (16.98)	54.34 (45.20)
Current at 3,300 N with joint movement, μA	0.648 (0.148)	0.357 (0.694)
Change in OCP† at 3,300 N with joint movement, mV‡	150.45 (60.78)	260.40 (48.42)
Current at 3,300 N with joint movement, μA	1.253 (0.386)	1.856 (1.023)
Change in OCP† at 3,300 N without joint movement, mV§	160.08 (40.08)	251.29 (45.39)
Current at 3,300 N without joint movement, μA	0.933 (0.185)	1.241 (0.585)

*Statistically significant difference (p = 0.009).
†Change in open circuit potential (OCP) measured relative to the at rest equilibrium level.
‡Statistically significant difference (p = 0.006).
§Statistically significant difference (p = 0.004).
SD, standard deviation.

change in OCP at 3,300 N with joint movement applied (260.40 mV (SD 48.42) vs 150.45 mV (SD 60.78); p = 0.006, ANOVA) and without joint movement applied (251.29 mV (SD 45.39) vs 160.08 mV (SD 40.08) ; p = 0.004, ANOVA) than 28 mm heads. No significant difference was found between 36 mm and 28 mm heads for corrosion current at 3,300 N with joint movement applied (1.856 μA (SD 1.023) vs 1.253 μA (SD 0.386); p = 0.206, ANOVA) or without joint movement applied (1.241 μA (SD 0.585) vs 0.933 μA (SD 0.18); p = 0.246, ANOVA).

Head sizes had no significant impact on corrosion current or change in OCP from rest to 100 N peak compression with joint movement, or once joint movement was stopped and 3,300 N cyclic compression was allowed to continue in the same test sequence. After pooling samples across head size, there was a significant increase in both corrosion current (-0.147 μA (SD 0.378) vs 0.356 μA (SD 0.428); p = 0.005, paired *t*-test) and

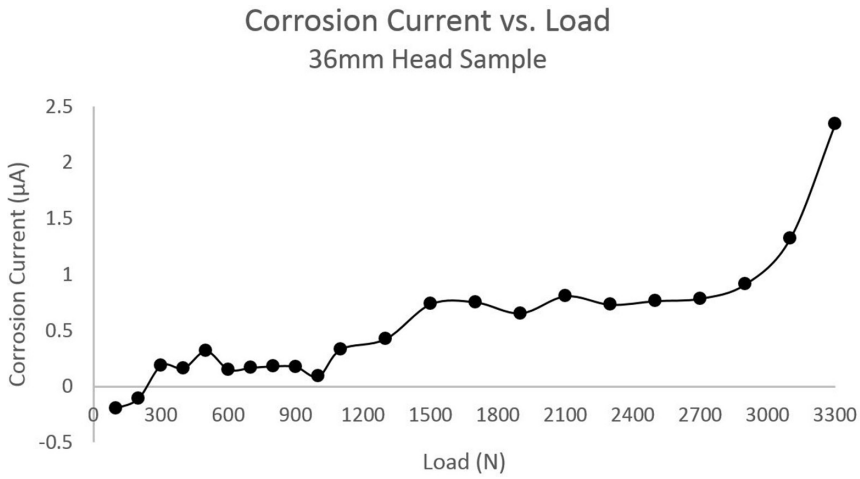

Fig. 7

Typical corrosion current vs. load plot for the incremental load test. This sample demonstrates a corrosion onset load of 1,500 N due to a marked increase in current compared to the baseline at lower loads.

t-test between the proximal and distal regions as well as heads versus stem tapers. Percentage areas of fretting and corrosion in the medial, lateral, posterior and anterior aspects were compared by ANOVA with Tukey post-hoc analysis. Data collected following wear cycling was analyzed by multiple linear regression to determine the effects of head size and loading regime (with or without joint movement). Statistical significance was determined to a level of 0.05.

Results

Results from the incremental load test are presented in Table I, and a typical corrosion current versus load plot is presented in Figure 7. Overall, 36 mm heads had significantly lower corrosion onset loads (1,250 N (SD 250) vs 1,800 N (SD 330) ; p = 0.009, ANOVA), significantly higher OCP (13.90 mV (SD 86.43) vs -24.21 mV (SD 87.39) ; p = 0.006 paired *t*-test) upon commencing joint movement and 100 N compression from rest. With pooled samples discontinuing joint movement at the 3300 N compression level significantly decreased corrosion current (1.554 μA (SD 0.801) vs 1.087 μA (SD 0.444); p = 0.042, paired *t*-test), but not OCP.

Visual inspection prior to testing found all devices free from defects and any visual signs of corrosion and wear. Qualitatively, stem trunnions showed no fretting damage and only small areas of mild corrosion as defined by Goldberg et al[15] for all of the trunnions paired with 36 mm heads and four of six with 28 mm heads. Head tapers showed greater damage than stem trunnions.

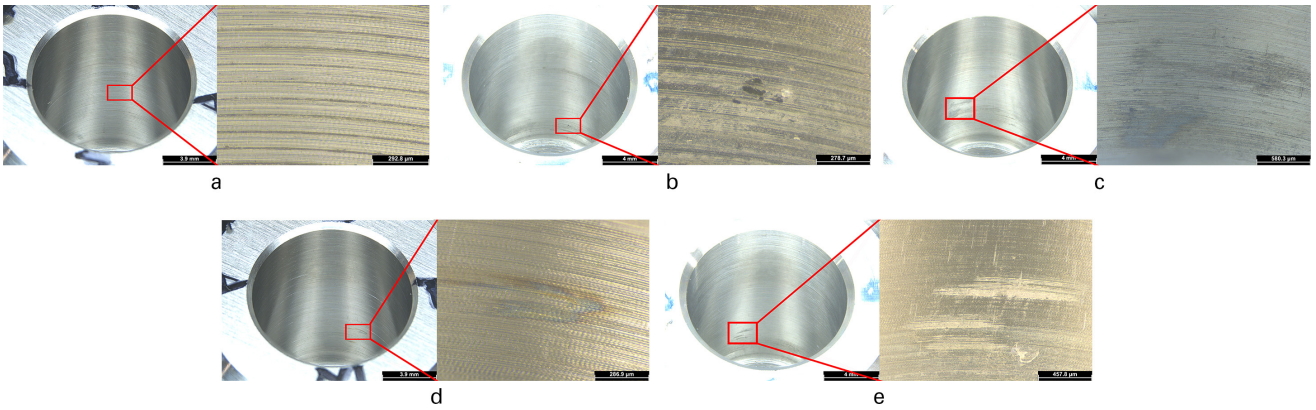

Fig. 8

Microscope images of head taper damage modes. a) Imprinting, b) pitting, c) darkened discoloration, d) 'oil-slick' discoloration, and e) fretting,

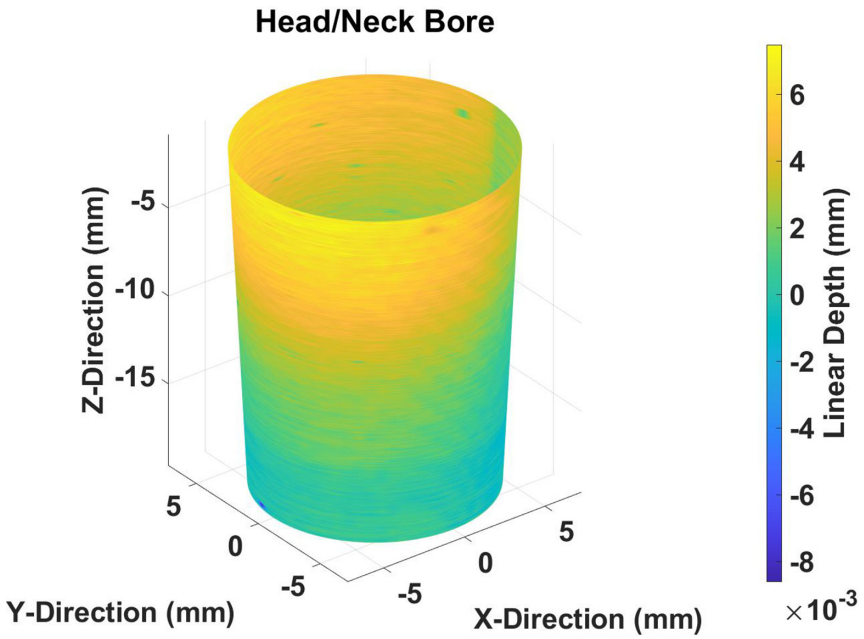

Fig. 9

Coordinate measuring machine wear map showing trend towards distal wear damage of head taper.

Heads tended to show greater corrosion than fretting damage. Only half of heads showed any fretting damage, constituting only small areas (< 3%). All heads showed mild corrosion damage. Only the most damaged head (36 mm, no joint movement group) met the Goldberg criteria[15] for moderate corrosion damage (> 30% discolored taper surface).

Head tapers exhibited imprinting (all samples), pitting (two of 36 mm heads, one of 28 mm heads), dark discoloration (four of 36 mm heads, no 28 mm heads), multicolored 'oil-slick' discoloration (four of 36 mm heads, one of 28 mm heads), and fretting (three of 36 mm heads, three of 28 mm heads) damage modes (Figure 8). All heads showed imprinting of trunnion microgrooves in the proximal head taper, extending distally 2 mm to 5 mm. CMM wear maps showed axisymmetric (2/12; 17%) and mirrored (5/12; 42%) wear patterns. The axisymmetric pattern typically showed a greater tendency for wear distally on the head taper (Figure 9). The mirrored wear pattern showed greater wear on diametrically opposed taper surfaces (Figure 10).

Head tapers had significantly greater proportions of their proximal than distal regions corroded (47% (SD 6%) vs 8% (SD 3%); $p < 0.001$). There was no significant difference in medial, lateral, anterior, or posterior fretting or corrosion scores.

Figure 11 presents the fretting and corrosion damage areas for head and stem tapers after wear cycling. Corrosion damage area was significantly greater for 36 mm heads (28% (SD 4%) vs 23 (SD 4%); $p = 0.050$, ANOVA). Fretting levels were low and no significant difference between head sizes was observed. Significantly greater

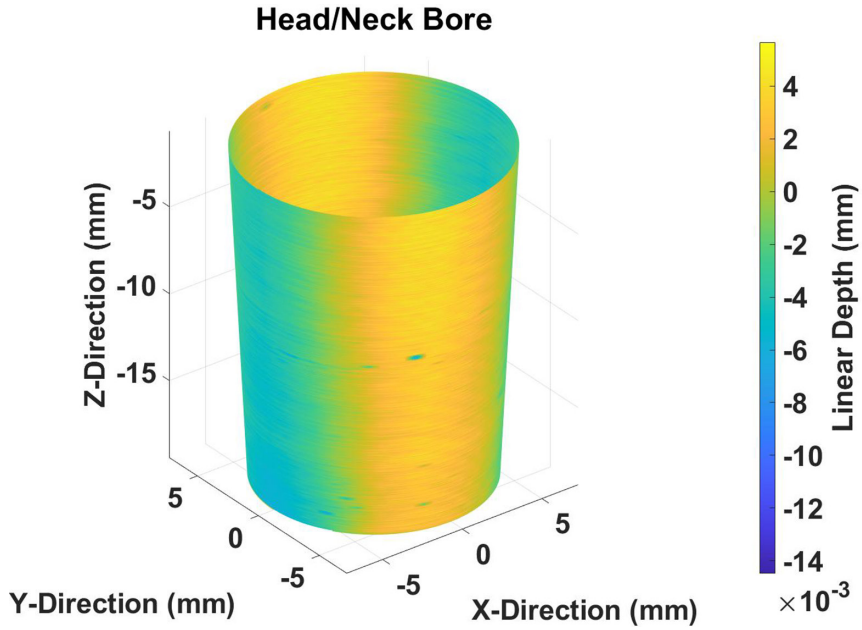

Fig. 10

Ccoordinate measuring machine wear map showing wear on diametrically opposed surfaces.

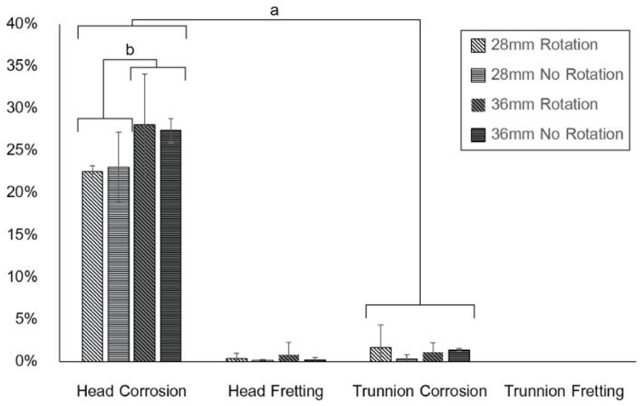

Fig. 11

Area percentage of corrosion and fretting damage after wear cycling. a) Significantly greater corrosion damage on head tapers than stem trunnions ($p < 0.001$), and b) significantly greater corrosion damage area for 36 mm over 28 mm heads ($p = 0.05$).

areas of head tapers were corroded than stems (25% (SD 4%) vs 1% (SD 1%); $p < 0.001$, ANOVA).

No significant difference in maximum linear wear depth was observed between 36 mm and 28 mm heads (4.49 µm (SD 3.21) vs 2.13 µm (SD 2.67); $p = 0.155$, ANOVA). Samples wear cycled with and without joint movement showed no significant difference in maximum linear wear depth (2.63 µm (SD 1.63) vs 3.99 µm (SD 3.45 µm); $p = 0.390$, ANOVA).

No statistically significant effect was found as a result of wear cycling with or without joint movement, nor were head size and joint movement found to be cofactors.

Discussion

The present study aimed to determine the role of joint movements in head-neck taper corrosion and differential performance between femoral head sizes in a highly controlled in vitro simulation. To date, mechanisms for the inferior corrosion resistance of larger femoral heads in some patient cohorts have been proposed following retrieval studies and finite element analyses. Retrieval studies provide direct clinical data on a particular patient cohort; however, the diverse populations they study limit precise assessment of a particular corrosion mechanism. Conversely, finite element analysis allows well controlled evaluation of particular mechanisms, but simplifications necessary for digitization may exclude important corrosion processes. The in vitro simulation presented here provides further insight into the corrosion performance of large femoral heads by closely estimating in-vivo conditions and allowing direct control of potentially confounding factors.

The test methods reproduced some taper wear and corrosion damage modes of components retrieved in-vivo, including imprinting, pitting, discoloration and fretting. Damage was generally mild but may have progressed if wear cycling continued considering corrosion damage has been found to progress with time in vivo.[15–17] Axisymmetric wear patterns were observed on the majority of head tapers, indicative of pistoning common with neutral offset heads.[9,18] The mirrored wear pattern is different from toggling type damage previously reported in retrieval studies.[19] Toggling type damage is exemplified by diagonally opposed damage areas,

whereas the mirrored damage pattern had diametrically opposed damage extending the full length of the taper. The axisymmetric and mirrored wear patterns may be the result manufacturing tolerances. Wade et al[20] measured the taper connections of commercially available stem and head tapers using CMM and found a maximum difference of 0.05° and 20 µm between samples from the same manufacturer and with the same design. While sample-to-sample variation is larger than that within a single sample, the axisymmetric and mirrored wear pattern depths (4 µm to 14 µm) are on the same order of magnitude as manufacturing tolerances. The femoral head's bore is typically manufactured on a lathe by rotating the femoral head around its axis of symmetry and translating a cutting head along the length of the bore. The axisymmetric pattern may be the result of imperfect translation of the cutter head and the mirrored pattern may be the result of imperfect rotation of the femoral head. Stem microgroove imprinting in the head's bore proximally was likely due to taper connection design. The Smith & Nephew-manufactured samples tested herein have a greater taper angle than their corresponding stem trunnion[21] leading to proximal contact within the head.

To our knowledge, this is the first reported electrochemical instrumentation of a hip simulator to measure taper corrosion related electrical activity. Previous taper corrosion studies using a hip simulator have measured wear by ion analysis, visual assessment, roughness measurement or gravimetric analysis.[22–24] Alternatively, electrochemical measurements have been made in models excluding full hip simulation, where instead the estimated torque is applied via a simplified apparatus.[8,25] Yan et al[26] instrumented a hip simulator to investigate corrosion in metal-on-metal hip arthroplasty articulation. They found that upon initiating hip simulation the OCP decreased by 70 mV, indicating a shift toward the material's active corrosion phase. Similarly, we found a small but significant increase in corrosion current (0.503 µA; $p = 0.005$) and decrease in OCP (38 mV; $p = 0.004$), indicative of electrochemical activity at the articular surface. This effect was observed under 100 N compression, well before taper corrosion initiated. The relative contribution of articular and taper corrosion could not be determined and could contribute to differences between head sizes. However, no significant difference between head sizes in corrosion current or change in OCP at the initiation of joint movement was observed, suggesting differences in articular surface electrochemical activity between head sizes were small if present.

Electrochemical measurements taken during the incremental load test in the short term indicate the effect of simulated gait induced frictional torque is significant. However, this did not translate to significant differences in taper damage after long term wear cycling. At 3,300 N peak compressive loading, corrosion current decreased by 30% once joint movement was stopped and 3,300 N cyclic compression was allowed to continue in the same test sequence. Farhoudi et al[27] performed a finite element analysis to investigate the effect of superimposing gait induced frictional moments over gait's compression. They found compression during gait largely dictated the connection mechanics, but frictional moments increased micromotion by 15%. Our study found frictional torque had no significant effect on taper damage after one million cycles.

Significant effect of head size and not the loading regime suggests that frictional torque is not the main mechanism involved in taper damage. However, this was found with a single bearing design, under restricted ROM and in pristine conditions. A portion of the larger head cohort's increased electrochemical activity (corrosion current, change in OCP) may be due to geometrical changes in the corrosion cell, such as reduced distance between the sample and reference or counter electrodes, or greater material engaged in the electrolytic solution due to the larger diameter. However, greater taper damage after cycling with larger heads indicates that the increased electrochemical activity is likely due at least in part to greater taper corrosion activity. We know that frictional torque scales with head diameter. Therefore, its contribution may increase with larger heads. The test apparatus used a conventional polyethylene socket with lower friction than modern cross-linked polyethylene[28] due to restricted availability of cross-linked material. The ROM was greatly reduced compared to in vivo gait; however, it is considered sufficient to induce frictional torque. In accordance with the Coulomb model of friction, the magnitude of frictional torque is not proportional to the ROM, it is only proportional to the friction coefficient and the normal force (compression) between the femoral head and acetabular liner. Therefore, the reduced ROM does not reduce the frictional torque. Pereira et al[5] retrieved metal-on-polyethylene components and found head diameter was an important co-factor with abrasive wear in predicting taper damage. Therefore, frictional torque may have a greater effect on taper corrosion with larger heads and higher friction bearings, particularly in the presence of third-body debris. A further study investigating worst case articular friction conditions is necessary to determine if the effect of frictional torque becomes significant when it is at its highest.

An alternative mechanism for the inferior corrosion resistance of larger heads may also be considered. Low-stem taper flexural rigidity has been identified as a factor increasing taper fretting corrosion in retrieved components.[16,29] Less stiff stem tapers are more susceptible to fretting displacements arising from elastic deformation. A taper flexed in bending experiences micromotion due to stretching on the bend's tensile side and shortening on the compression side.[30] The same mechanism may be relevant to the tapered bore of the head.

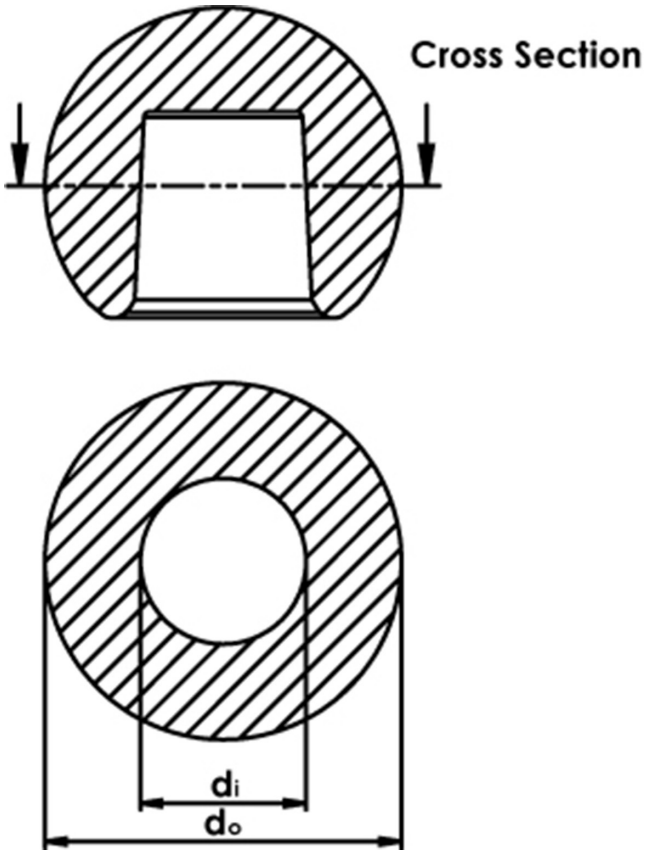

Fig. 12

Cross section of the femoral head through the taper, identifying the inner diameter (di) taken as the taper diameter, and outer diameter (do) taken as the articular diameter.

Flexural rigidity is calculated by multiplying the second moment of area by the elastic modulus.[15] The cross-section of the femoral head through the bore is a ring (Figure 12). The flexural rigidity of the cross-section of the femoral head through the bore may be calculated by the equation below.[31]

$$\textit{Flexural Rigidity} = E \times I = E \times \frac{\pi}{64}\left(d_o^4 - d_i^4\right)$$

Where E is the elastic modulus, I is the second moment of area, d_o is the outer diameter and d_i is the inner diameter. The elastic modulus of CoCr is 210 GPa.[32] The inner and outer diameter vary along the length of the bore. For the purposes of approximation, the outer diameter may be taken as the femoral head's spherical diameter and the inner diameter may be taken as the proximal diameter of the bore (12 mm) since the subject taper connection was designed for proximal engagement. The flexural rigidity for a 28 mm head is then calculated as 6,100 Nm^2 and for the 36 mm head as 17,100 Nm^2. The flexural rigidity of the femoral head bore for the 36 mm head is 2.8 times that of the 28 mm head. Kao et al[33] found stem taper fretting inversely related to stem taper flexural rigidity in a retrieval analysis of 77 metal-on-polyethylene THA implants. The highest flexural rigidity of the tapers in this study was 3.5-times higher than the lowest. The relative difference in stem taper flexural rigidity found significant in the study by Kao et al[23] (3.5-times) is similar in magnitude to the relative difference in femoral head bore flexural rigidity of the samples in the present study (2.8-times), suggesting the magnitude of differences in flexural rigidity of the femoral head bore due to femoral head size may be at significant levels. To the knowledge of the authors, previous studies have investigated the flexural rigidity of the stem taper but not the femoral bore.

Elastic deformation induced micromotion would be minimized if the head's bore and stem's trunnion had equal stiffness due to proportional bending without relative motion. Mating similar metals, such as with CoCr head-stem pairs, approximates this scenario. Conversely with dissimilar metal pairs, CoCr alloy is twice as stiff as titanium alloy (210 to 253 GPa vs 100 to 110 GPa, respectively).[32] Dissimilar metals with dissimilar stiffness increase the flexural rigidity differential, resulting in greater elastic deformation induced relative motion. Retrieval analyses have shown that dissimilar metal head-stem pairs have greater taper damage than same metal combinations.[6,15,34–36] It is difficult to isolate mechanical and electrochemical contributions due to galvanic corrosion, but differential flexural rigidity may explain these findings under the phenomena of mechanically assisted crevice corrosion without galvanic corrosion. With larger heads, the flexural rigidity differential is increased by stiffening the head's tapered bore. Increasing head size increases the tapered bore's wall thickness thus increasing its flexural rigidity. As a result, larger heads have a greater flexural rigidity differential leading to greater elastic deformation induced micromotion and potentially greater taper wear damage. Further research is necessary to investigate this proposed mechanism.

Limitations. This study is subject to limitations. The effect of frictional torque may not have been observed due to low study power (< 40%) and the specific test methods employed. Addition of joint movement to induce frictional torque did not significantly increase taper wear damage. This suggests that under pristine metal-on-polyethylene wear conditions, frictional torque is not the main contributor to the inferior taper corrosion resistance of larger heads. The findings herein may not extrapolate to adverse wear conditions where frictional torque may increase.

The study is further limited by practical simplifications necessary for completion, such as reduced ROM, limited cycling duration and exclusion of biological factors. ROM and cycling duration was limited to allow practical test frequency and study duration. ROM is considered sufficient to induce frictional torque; however, discontinuing cycling at one million cycles may exclude clinically relevant taper corrosion. Mechanically-assisted

crevice corrosion increases in severity with time as a corrosive environment builds within the taper connection,[37] as observed in multiple retrieval studies.[15–17] One million steps simulates only a year's usage,[38] but corrosion levels necessitating revision may take five to seven years to develop.[39,40] However, damage modes consistent with retrieved components,[41,42] including pitting and imprinting, were observed in this study. Testing was performed in PBS instead of a biological lubricant, which may affect frictional torque. Testing in PBS was selected to align and allow comparison with similar in vitro taper connection tribocorrosion studies.[9,43–45] Further, the test apparatus held the components in an inverted position, which may have caused third body wear due to debris entrapment within the taper connection.

The study is limited to a single prosthesis design. Aspects of prosthesis design, such as head offset, head material, and taper connection geometry were not subject to investigation. Head offset has been identified as an important factor affecting taper corrosion;[9,46,47] however, neutral offset heads were selected for testing to control for head offset and taper coverage, and to isolate the effect of head size. Retrieval analyses have found taper design is an important factor related to tribocorrosion.[48] Retrieval analyses have found femoral stems with lower neck flexural rigidity,[15,49] lower taper flexural rigidity,[16,29,33] higher taper roughness,[50] lower taper angle,[33] and narrower tapers[17] associated with greater susceptibility to tribocorrosion. Ceramic heads have also been found in retrieval studies to be less susceptible to tribocorrosion than metal heads.[17,49,51,52] Head offset, taper design, and femoral head and stem material were controlled variables in this study to isolate the effect of head size with a CoCr head. Higher loads than those tested may be experienced during stumbling or stair climb;[53] however, gait representative loads were selected since these loads more commonly recur over time. The findings presented herein represent only the particular prostheses and conditions tested, and may not translate to different devices and conditions.

Conflicting evidence related to the effect of head size on tribocorrosion susceptibility has been reported elsewhere. Dyrkacz et al[4] found significantly greater severity and area of taper corrosion and fretting damage with 36 mm than 28 mm heads in a retrieval study of 74 metal-on-polyethylene hip arthroplasty implants. Conversely, in a similar retrieval analysis of 154 metal-on-polyethylene hip arthroplasty implants, Triantafyllopoulos et al[6] found no significant difference between head sizes in fretting or corrosion severity. Hip arthroplasty implant factors, such as head lateral offset, head material, and taper geometry, must be considered, alongside head diameter to balance the risk related to taper tribocorrosion and other implant-related failure modes. However, the present study supports the recommendations of a recent consensus statement released by the American Association of Hip and Knee Surgeons, the American Academy of Orthopaedic Surgeons, and The Hip Society[54] that a large diameter CoCr femoral head is a moderate- to high-risk implant factor for head-neck taper corrosion associated adverse local tissue reactions following metal-on-polyethylene THA.

In conclusion, larger femoral heads in simulated hip arthroplasty were found more susceptible to taper corrosion, and contrary to the hypothesis herein, frictional torque in a pristine metal-on-polyethylene bearing was not supported as the underlying mechanism. Frictional torque may have a greater effect with adverse wear conditions. Further investigation of alternative mechanisms, such as increased flexural rigidity differential, is required to understand the inferior performance of larger heads and its clinical significance.

Take home message

- Larger femoral heads were found more susceptible to head-neck taper tribocorrosion in an instrumented hip simulator.
- However, the increased tribocorrosion was not due to increased frictional torque, in pristine conditions. Therefore, larger femoral heads increase the risk of head-neck taper tribocorrosion, even under pristine conditions.

References

1. **Crowninshield RD**, **Maloney WJ**, **Wentz DH**, **Humphrey SM**, **Blanchard CR**. Biomechanics of large femoral heads: what they do and don't do. *Clin Orthop Relat Res. 429*:102–107.
2. **Langton DJ**, **Sidaginamale R**, **Lord JK**, **Nargol AVF**, **Joyce TJ**. Taper junction failure in large-diameter metal-on-metal bearings. *Bone Joint Res.* 2012;1(4):56–63.
3. **Silverman EJ**, **Ashley B**, **Sheth NP**. Metal-on-metal total hip arthroplasty: is there still a role in 2016? *Curr Rev Musculoskelet Med.* 2016;9(1):93–96.
4. **Dyrkacz RMR**, **Brandt J-. M**, **Ojo OA**, **Turgeon TR**, **Wyss UP**. The influence of head size on corrosion and fretting behaviour at the head-neck interface of artificial hip joints. *J Arthroplasty.* 2013;28(6):1036–1040.
5. **Pereira X**, **Moga I**, **Harrington MA**, **Patel PD**, **Ismaily SK**, **Noble PC**. Variables influencing tribo-corrosion of modular junctions in metal-on- polyethylene THR. 2014. https://www.ors.org/Transactions/60/1832.pdf (date last accessed 27 September 2021).
6. **Triantafyllopoulos GK**, **Elpers ME**, **Burket JC**, **Esposito CI**, **Padgett DE**, **Wright TM**. Otto aufranc award: large heads do not increase damage at the head-neck taper of metal-on-polyethylene total hip arthroplasties. *Clin Orthop Relat Res.* 2016;474(2):330–338.
7. **Craig P**, **Bancroft G**, **Burton A**, **Collier S**, **Shaylor P**, **Sinha A**. Raised levels of metal ions in the blood in patients who have undergone uncemented metal-on-polyethylene Trident-Accolade total hip replacement. *Bone Joint J.* 2014;96-B(1):43–47.
8. **Jauch SY**, **Coles LG**, **Ng LV**, **Miles AW**, **Gill HS**. Low torque levels can initiate a removal of the passivation layer and cause fretting in modular hip stems. *Med Eng Phys.* 2014;36(9):1140–1146.
9. **Gilbert JL**, **Mehta M**, **Pinder B**. Fretting crevice corrosion of stainless steel stem-CoCr femoral head connections: comparisons of materials, initial moisture, and offset length. *J Biomed Mater Res B Appl Biomater.* 2009;88(1):162–173.
10. **International Organization for Standardization**. ISO 7206-10:2003 Implants for surgery - partial and total hip-joint prostheses - part 10: determination of resistance to static load of modular femoral heads. Switzerland: International Organization for Standardization. 2003.
11. **International Organization for Standardization**. ISO 14242-1: Implants for surgery - wear of total hip-joint prostheses - part 1: loarding and displacement parameters for wear-testing machines and corresponding environmental conditions for test. 2014. https://www.iso.org/standard/63073.html (date last accessed 27 September 2021).
12. **ASTM International**. ASTM F1875 - 98(2014) In: Standard practice for fretting corrosion testing of modular implant interfaces: hip femoral head-bore and cone taper

interface. <span class=" refpublisherloc"="">West Conshohocken, Philadelphia, USA: 1998.
13. **Brown S**, **Abera A**, **D'Onofrio M**, **Flemming C**. Effects of neck extension, coverage, and frequency on the fretting corrosion of modular THR bore and cone interface. In: Marlowe D, Parr J, Mayor M, eds. *Modularity of Orthopedic Implants*. West Conshohocken, Philadelphia, USA: ASTM International, 1997: 189–198.
14. **Mihalko W**. Using coordinate measuring machine validated with white light interferometry to identify contributors to material loss due to corrosion of total hip replacement modular junctions. West Conshohocken, Philadelphia, USA: ASTM International. 2018: 118–130.
15. **Goldberg JR**, **Gilbert JL**, **Jacobs JJ**, **Bauer TW**, **Paprosky W**, **Leurgans S**. A multicenter retrieval study of the taper interfaces of modular hip prostheses. *Clinical Orthopaedics and Related Research*. 2002;401:149–161.
16. **Higgs GB**, **MacDonald DW**, **Gilbert JL**, **Rimnac CM**, **Kurtz SM**, **Implant Research Center Writing Committee**. Does Taper size have an effect on taper damage in retrieved metal-on-polyethylene total hip devices? *J Arthroplasty*. 2016;31(9 Suppl):277–281.
17. **Tan SC**, **Lau ACK**, **Del Balso C**, **Howard JL**, **Lanting BA**, **Teeter MG**. Tribocorrosion: Ceramic and oxidized zirconium vs cobalt-chromium heads in total hip arthroplasty. *J Arthroplasty*. 2016;31(9):2064–2071.
18. **Morlock MM**, **Dickinson EC**, **Günther K-P**, **Bünte D**, **Polster V**. Head Taper corrosion causing head bottoming out and consecutive gross stem taper failure in total hip arthroplasty. *J Arthroplasty*. 2018;33(11):3581–3590.
19. **Bishop N**, **Witt F**, **Pourzal R**, **et al**. Wear patterns of taper connections in retrieved large diameter metal-on-metal bearings. *J Orthop Res*. 2013;31(7):1116–1122.
20. **Wade A**, **Beadling AR**, **Neville A**, **et al**. Geometric variations of modular head-stem taper junctions of total hip replacements. *Med Eng Phys*. 2020;83:34–47.
21. **Mueller U**, **Braun S**, **Schroeder S**, **Sonntag R**, **Kretzer JP**. Same same but different? 12/14 stem and head tapers in total hip arthroplasty. *J Arthroplasty*. 2017;32(10):3191–3199.
22. **Bhalekar RM**, **Smith SL**, **Joyce TJ**. Hip simulator testing of the taper-trunnion junction and bearing surfaces of contemporary metal-on-cross-linked-polyethylene hip prostheses. *J Biomed Mater Res*. 2019;108(1):156–166.
23. **Bhalekar RM**, **Smith SL**, **Joyce TJ**. Wear at the taper-trunnion junction of contemporary ceramic-on-ceramic hips shown in a multistation hip simulator. *J Biomed Mater Res*. 2018;107(4):1199–1209.
24. **Kyomoto M**, **Shoyama Y**, **Saiga K**, **Moro T**, **Ishihara K**. Reducing fretting-initiated crevice corrosion in hip simulator tests using a zirconia-toughened alumina femoral head. *J Biomed Mater Res*. 2018;106(8):2815–2826.
25. **Panagiotidou A**, **Bolland B**, **Meswania J**, **Skinner J**, **Haddad F**, **Hart A**, **et al**. Effect of increased frictional torque on the fretting corrosion behaviour of the large diameter femoral head. poster 0184, ors annu meet. New Orleans, LA. 2014.
26. **Yan Y**, **Neville A**, **Dowson D**, **Williams S**, **Fisher J**. Electrochemical instrumentation of a hip simulator: a new tool for assessing the role of corrosion in metal-on-metal hip joints. *Proc Inst Mech Eng H*. 2010;224(11):1267–1273.
27. **Fallahnezhad K**, **Farhoudi H**, **Oskouei RH**, **Taylor M**. A finite element study on the mechanical response of the head-neck interface of hip implants under realistic forces and moments of daily activities: Part 2. *J Mech Behav Biomed Mater*. 2018;77:164–170.
28. **Burroughs BR**, **Muratoglu OK**, **Bragdon CR**, **Wannomae KK**, **Christensen S**, **Lozynsky AJ**. In vitro comparison of frictional torque and torsional resistance of aged conventional gamma-in-nitrogen sterilized polyethylene versus aged highly crosslinked polyethylene articulating against head sizes larger than 32 mm. *Acta Orthop. ;77*(5):710–718. n.d.
29. **Arnholt C**, **Underwood R**, **Macdonald DW**, **Higgs GB**, **Chen AF**, **Klein G**, **et al**. Microgrooved surface topography does not influence fretting corrosion of tapers in total hip arthroplasty: classification and retrieval. Analysis AS, editor. West Conshohocken, Philadelphia, USA: ASTM International. 2015.
30. Eliaz N, editor. Medical implant corrosion: electrochemistry at metallic biomaterial surface. New York, New York, USA: Springer. 2012: 1–28.
31. **Juvinall RC**, **Marshek KM**. *Fundamentals of Machine Component Design*. 4th ed. Hoboken, New Jersey, USA: John Wiley & Sons. 2006.
32. **Murphy W**, **Black J**, **Hastings G**. *Handbook of Biomaterial Properties*. 2nd ed. New York, New York: Springer. 2016.
33. **Kao Y-YJ**, **Koch CN**, **Wright TM**, **Padgett DE**. Flexural rigidity, taper angle, and contact length affect fretting of the femoral stem trunnion in total hip arthroplasty. *J Arthroplasty*. 2016;31(9 Suppl):254–258.
34. **Collier J**, **Surprenant V**, **Jensen RE**, **Mayor MB**, **Surprenant HP**. Corrosion between the components of modular femoral hip prostheses. *J Bone Joint Surg Br*. 1992;74-B(4):511–517.
35. **Collier J**, **Mayor M**, **Jensen RE**, **Surprenant VA**, **Surprenant HP**, **McNamara JL**, **et al**. Mechanisms of failure of modular prostheses. *Clin Orthop Relat Res*. ;285:129–139.
36. **Cook SD**, **Barrack RL**, **Baffes GC**, **Serekian P**, **Dong N**, **et al**. Wear and corrosion of modular interfaces in total hip replacements. *Clin Orthop Relat Res*. 298:80–88.
37. Marlowe D, Parr J, Mayor M, editors. The mechanical and electrochemical processes associated with taper fretting crevice corrosion: a review. Philadelphia, USA: ASTM International. 1997: 45–59.
38. **Schmalzried TP**, **Szuszczewicz ES**, **Northfield MR**, **et al**. Quantitative assessment of walking activity after total hip or knee replacement*. J Bone Joint Surg Am. 1998;80-A(1):54–59.
39. **Tan S**, **Teeter M**, **Del BC**, **Howard J**, **Lanting B**. Effect of taper design on trunnionosis in metal on polyethylene total hip arthroplasty. *J Arthroplasty*. 2018;33(10):3231–3237.
40. **Persson A**, **Eisler T**, **Bodén H**, **Krupic F**, **Sköldenberg O**, **Muren O**. Revision for symptomatic pseudotumor after primary metal-on-polyethylene total hip arthroplasty with a standard femoral stem. *J Bone Joint Surg Am*. 2018;100-A(11):942–949.
41. **Gilbert JL**, **Buckley CA**, **Jacobs JJ**. In vivo corrosion of modular hip prosthesis components in mixed and similar metal combinations. The effect of crevice, stress, motion, and alloy coupling. *J Biomed Mater Res*. 1993;27(12):1533–1544.
42. **Arnholt CM**, **MacDonald DW**, **Underwood RJ**, **et al**. Do stem taper microgrooves influence taper corrosion in total hip arthroplasty? a matched cohort retrieval study. *J Arthroplasty*. 2017;32(4):1363–1373.
43. **Ouellette ES**, **Mali SA**, **Kim J**, **Grostefon J**, **Gilbert JL**. Design, material, and seating load effects on in vitro fretting corrosion performance of modular head-neck tapers. *J Arthroplasty*. 2019;34(5):991–1002.
44. **Pierre D**, **Swaminathan V**, **Scholl LY**, **TenHuisen K**, **Gilbert JL**. effects of seating load magnitude on incremental cyclic fretting corrosion in 5°40′ mixed alloy modular taper junctions. J Arthroplasty. 2018;33(6):1953–1961.
45. **Rowan FE**, **Wright TM**, **Padgett DE**. The onset of fretting at the head-stem connection in hip arthroplasty is affected by head material and trunnion design under simulated corrosion conditions. *J Orthop Res*. 2018;36(6):1630–1636.
46. **Del Balso C**, **Teeter MG**, **Tan SC**, **Lanting BA**, **Howard JL**. Taperosis: Does head length affect fretting and corrosion in total hip arthroplasty? *Bone Joint J*. 2015;97-B(7):911–916.
47. **Donaldson FE**, **Coburn JC**, **Siegel KL**. Total hip arthroplasty head-neck contact mechanics: a stochastic investigation of key parameters. *J Biomech*. 2014;47(7):1634–1641.
48. **Tan SC**, **Teeter MG**, **Del Balso C**, **Howard JL**, **Lanting BA**. Effect of taper design on trunnionosis in metal on polyethylene total hip arthroplasty. J Arthroplasty. 2015;30(7):1269–1272.
49. **Kurtz SM**, **Kocagöz SB**, **Hanzlik JA**, **et al**. Do ceramic femoral heads reduce taper fretting corrosion in hip arthroplasty? A retrieval study. Clin Orthop Relat Res. 2013;471(10):3270–3282.
50. **Pourzal R**, **Hall DJ**, **Ha NQ**, **et al**. Does surface topography play a role in taper damage in head-neck modular junctions? Clin Orthop Relat Res. 2016;474(10):2232–2242.
51. **Huot Carlson JC**, **Van Citters DW**, **Currier JH**, **Bryant AM**, **Mayor MB**, **Collier JP**. Femoral stem fracture and in vivo corrosion of retrieved modular femoral hips. J Arthroplasty. 2012;27(7):1389-1396..
52. **Klunklin K**, **Schmidt CM**, **Roy ME**, **Whiteside LA**. Fretting and corrosion damage at the head-neck taper Is reduced with ceramic femoral heads: A retrieval study: Poster 1143, Orthopaedic Research Society. New Orleans, Louisiana, USA, 2014.
53. **Bergmann G**, **Graichen F**, **Rohlmann A**, **et al**. Realistic loads for testing hip implants. *Biomed Mater Eng*. 2010;20(2):65–75.
54. **Kwon YM**, **Della VC**, **Garbuz DS**, **Berry DJ**, **Jacobs JJ**. Risk stratification algorithm for management of head-neck taper tribocorrosion in patients with metal-on-polyethylene total hip arthroplasty: Consensus statement of the American Association of Hip and Knee Surgeons, American Association of Hip and Knee Surgeons, the American Academy of Orthopaedic Surgeons, and The Hip Society. *J Bone Joint Surg Am*. 103-A(5):1–9.

Author information:
- C. M. Wight, PhD, Graduate Student, Institute of Biomedical Engineering, University of Toronto, Toronto, Ontario, Canada.
- C. M. Whyne, PhD, Director, Orthopaedic Biomechanics Laboratory, Sunnybrook Research Institute, Toronto, Ontario, Canada.
- E. R. Bogoch, MD, FRCSC, Brookfield Chair in Fracture Prevention, Department of Surgery, University of Toronto, Brookfield Chair in Fracture Prevention, Toronto, Ontario, Canada.
- R. Zdero, PhD, Professor
- R. M. Chapman, PhD, Lecturing Professor

London Health Science Centre, Western University, London, Ontario, Canada.
- D. W. van Citters, PhD, Associate Professor, Thayer School of Engineering at Dartmouth College, Western University, Hanover, New Hampshire, USA.
- W. R. Walsh, PhD, Director, Surgical and Orthopaedic Research Laboratory, UNSW Prince of Wales Clinical School, Randwick, New South Wales, Australia.
- E. Schemitsch, MD, FRCSC, Chair/Chief, Division of Orthopaedic Surgery, Department of Surgery, Schulich School of Medicine and Dentistry, University of Western Ontario, London, Ontario, Canada.

Author contributions:
- C. M. Wight: Conceptualization, Formal analysis, Funding acquisition, Investigation, Methodology, Project administration, Writing – original draft.
- C. M. Whyne: Conceptualization, Supervision, Writing - reviewing and editing.
- E. R. Bogoch: Conceptualization, Supervision, Writing - reviewing and editing.
- R. Zdero: Conceptualization, Supervision, Writing - reviewing and editing.
- R. M. Chapman: Methodology, Formal analysis, Writing - reviewing and editing.
- D. W. van Citters: Methodology, Formal analysis, Resources, Writing - reviewing and editing.
- W. R. Walsh: Methodology, Project administration, Resources, Writing - reviewing and editing.
- E. Schemitsch: Conceptualization, Funding acquisition, Resources, Supervision, Writing - reviewing and editing.

Funding statement:
- No benefits in any form have been received or will be received from a commercial party related directly or indirectly to the subject of this article

ICMJE COI statement:
- C. Wight reports a grant from NSERC, which is related to this work, and employment from Corin, which is unrelated. D. Van Citters reports consultancy for Anika; and grants/grants pending from DePuy Synthes Joint Reconstruction, RevBio, amd ConforMIS; and payment for development of educational presentations from Medacta, all of which is unrelated to this work. E. Schemitsch declares consultancy for Smith & Nephew, Stryker, Depuy Synthes, Acumed, Sanofi, ITS, Swemac, Amgen, and Medtronic; grants/grants pending from Biocomposites; royalties from Stryker; and research support from Stryker, Smith & Nephew, Depuy Synthes, and Zimmer, all of which is unrelated to this article. W. Walsh reports consultancy and royalties from SeaSpine, which is unrelated. R. Zdero reports royalties from Elsevier annd ERC Press; and research support from Sawbones, Stryker, Zimmer, and Smith & Nephew, all of which is also unrelaed to this article.

Open access funding
- The authors report that this work was supported by Smith & Nephew, USA.